REPORT DOCUMENTATION PAGE

Form Approved
OMB No. 0704-0188

1. REPORT DATE *(DD-MM-YYYY)*	2. REPORT TYPE	3. DATES COVERED *(From - To)*
23-04-2015	Final	11/06/11 -- 30/05/14

4. TITLE AND SUBTITLE
Experiments in Developing Wakes

5a. CONTRACT NUMBER
N00014-11-1-0553

5b. GRANT NUMBER

5c. PROGRAM ELEMENT NUMBER

6. AUTHOR(S)
Spedding, Geoffrey R.

5d. PROJECT NUMBER

5e. TASK NUMBER

5f. WORK UNIT NUMBER

7. PERFORMING ORGANIZATION NAME(S) AND ADDRESS(ES)
G.R. Spedding
Department of Aerospace & Mechanical Engineering
University of Southern California
University Park Campus, Los Angeles, CA 90089-1453

8. PERFORMING ORGANIZATION REPORT NUMBER

9. SPONSORING/MONITORING AGENCY NAME(S) AND ADDRESS(ES)
Dr. R. Joslin
Office of Naval Research
800 North Quincy Street
Ballston Tower One
Arlington, VA 22217-5000

10. SPONSOR/MONITOR'S ACRONYM(S)

11. SPONSOR/MONITOR'S REPORT NUMBER(S)

12. DISTRIBUTION/AVAILABILITY STATEMENT

13. SUPPLEMENTARY NOTES

14. ABSTRACT

A three-year program (with no cost extension through Deeember 2014) was completed with 3 primary objeetives: (1) To develop a robust refractive index matched method for time-resolved PIV measurements of early wakes in a stably-stratified fluid. (2) To use this technique to investigate one example of an early wake with new analysis methods. (3) To compare results with numerical simulations. Objectives (1) and (2) were completed and showed that previous ideas on universal and 3D initial conditions were not realistic. The ways in which this finding complicates generalization of ONR-relevant conditions is not yet clear. The objective#3 is in process. Significant progress has been made in DMD descriptions of the experimental data, in readiness for similar modal comparisons in simulations. Simulations have been prepared and run in OpenFOAM. The implementation in Star/CCM+ is not simple (despite our extensive inside contacts at the company), but progress is being made.

15. SUBJECT TERMS
Stratified wakes, self-propelled bodies, turbulence decay, signature detection.

16. SECURITY CLASSIFICATION OF:			17. LIMITATION OF ABSTRACT	18. NUMBER OF PAGES	19a. NAME OF RESPONSIBLE PERSON
a. REPORT	b. ABSTRACT	c. THIS PAGE			Geoffrey Spedding
U	U	U	UU	11	19b. TELEPHONE NUMBER *(Include area code)* 213 740 4132

20150504021

USC Viterbi
School of Engineering

AEROSPACE AND MECHANICAL ENGINEERING
Geoffrey Spedding
Professor, Chair

April 23rd 2015

To whom it may concern,

Please find enclosed a copy of our final report on ONR contract# N00014-11-1-0553.

I am happy to answer any questions arising, and can be reached at any of the contact points below, and most rapidly at geoff@usc.edu

Yours sincerely,

G. R. Spedding
Professor and Chair
Department of Aerospace and Mechanical Engineering

University of Southern California
3650 McClintock Ave., Los Angeles, California 90089-1453 • Tel: 213 740 4132 • Fax: 213 740 8071

Final Report

for

Experiments in Developing Wakes

ONR Contract# N00014-11-1-0553

Office of Naval Research
800 North Quincy Street
Ballston Tower One
Arlington, VA 22217-5000
Attn: Dr R. Joslin

Submitted by:

Geoffrey R Spedding
Professor

Submission date: April 27, 2014

Department of Aerospace & Mechanical Engineering
University of Southern California
Los Angeles, CA 90089-1191
Phone: (213) 740-4132
Fax: (213) 740-8071

1. Summary of project objectives

A summary of the technical objectives outlined in the original proposal is given below:

Based on the argument that we know much about stratified wakes in the non-equilibrium and far-wake regimes, but little about their initial formation, the technical objectives were to conduct a new series of experiments on early/near wakes in a stably-stratified environment. The detailed technical objectives are twofold:

(i) To investigate the flow field at early times so as to find when turbulent motions are affected by stratification, and how;

(ii) To carefully compare laboratory measurements with equivalent numerical experimental data. The purpose will be to use not only high-resolution, state-of-the-art schemes, but also standard commercial codes to see whether they are of any use in parametric studies. If so, then ONR-relevant comparisons may be run rapidly on varying geometries.

Background

This background material has been discussed before, but is provided in case a new reader is unfamiliar with the abbreviated objectives above.

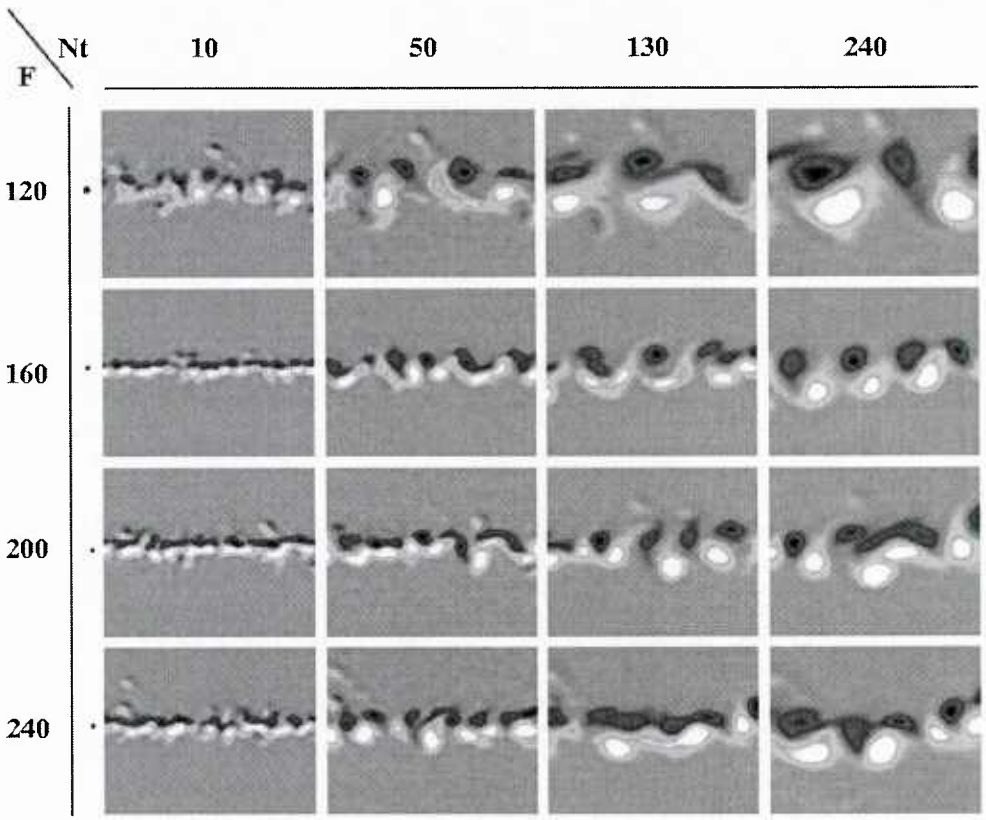

Fig. 1. The time evolution of vertical vorticity, from Nt = 10-240, at high Fr. Most laboratory experiments are conducted for Fr < 10. Here, results are directly applicable to Navy interests.

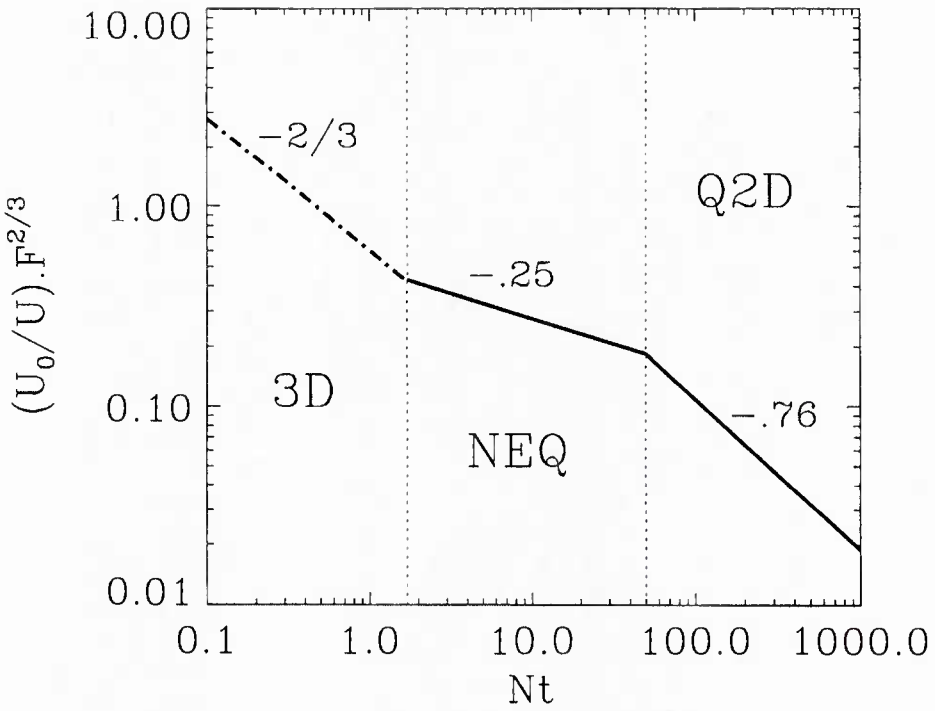

Fig. 2. The universal scaling for nonzero-momentum wakes, where F is an effective Froude number based on a length scale calculated from the wake momentum defect.

Fig. 1 shows 4 time series of the vertical vorticity in a developing wake behind towed spheres, with increasing Froude number down the vertical axis. Though the initial conditions are quite disordered, all wakes eventually converge to a quite stable and persistent pattern of alternating sign vortices. All the Froude numbers in Fig. 1 are rather high compared with most laboratory experiments, and the last one of Fr = 240 is representative of ONR conditions. We concluded that even ONR-relevant applications would be likely to develop wake patterns like this.

The result was very robust, independent of details of the body shape and even whether or not it was self-propelled. A simple rescaling based on measured or estimated drag coefficient could collapse all data onto curves such as Fig. 2. The results were divided into 3 regimes. An initial presumed 3D regime is followed by a non-equilibrium stage (NEQ) where the turbulent flow adjusts to the background density gradient. It is this stage where kinetic energy densities are unusually high and which show the wake assuming its particular form that later proves to be stable and long-lasting. In the final stages (Q2D), the flow evolves with very little vertical motion, as if it were on 2D planes. However, the dynamics are not at all 2D because the energy decay is strongly affected by vertical shearing motion between decoupled layers.

All of the actual evidence behind this plot is shown in the solid lines, confined to the NEQ and Q2D regimes. There have been no actual observations in the 3D regime because hitherto optically-based methods such as PIV have not been able to penetrate this domain as the strong

local density gradients cause variation in refractive index that themselves can be mistaken for turbulence. The main purpose of these experiments is to apply new measurement methods in refractive index matched fluids to access this early wake. The effort has been completely successful.

2. Technical approach

A. Laboratory experiments

Two improved capabilities were added to allow access in experiments to the postulated 3D regime of Fig. 1. First, since there is no anisotropy in the flow, all three velocity components must be acquired simultaneously, so that reasonably comprehensive statistics can be obtained. The new experiments use moderate frame rate (50 Hz) acquisition of stereo-PIV data behind the wake-generator (a sphere or grid) to obtain 3 velocity components in selected planes, and hence all components of the Reynolds stress tensor (though not all components of the dissipation rate tensor). The second modification is to use refractive index-matched fluids so that variations in density are not matched by variations in refractive index. This is accomplished using carefully measured mixtures of salt and ethanol solutions. For the first time, turbulent motions close to the point of origin in a stratified fluid have been measured in the wake flows.

B. Numerical simulations

USC experiments have spurred a number of competing numerical solutions, all of which can be shown to match the late wake results with satisfactory detail. However, in every case, the initial conditions must be very carefully tuned and/or selected so that the expected evolution rates occur. They are therefore not truly independent. New experiments have non-uniform grid spacings and can include the body itself (Fig. 3) but the need for selection of initial conditions at anything other than low Re is still evident.

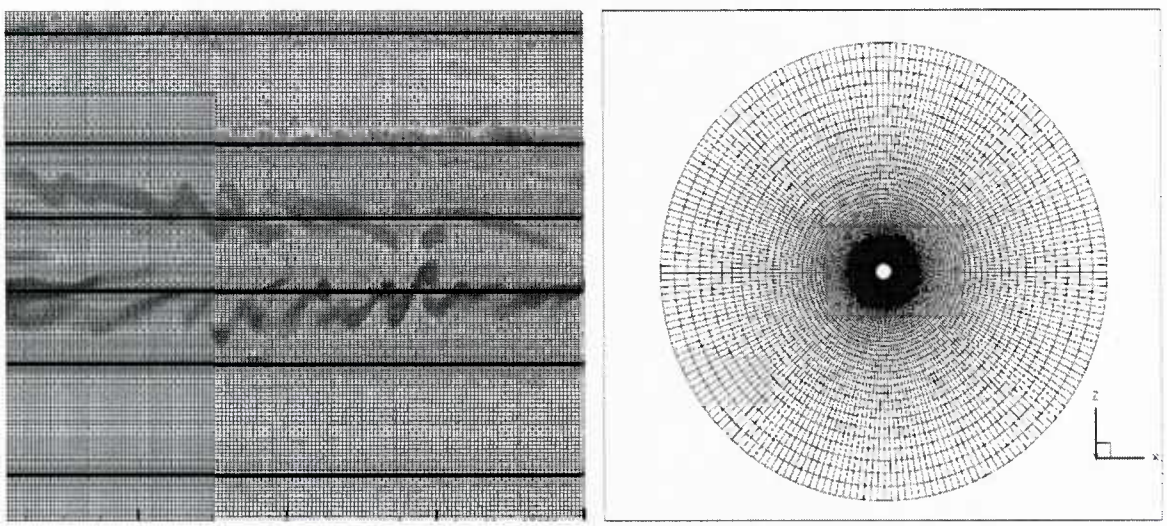

Fig. 3: Numerical simulation grids of Diamessis (left) who eoneentrated on the NEQ wake regime and its secondary instabilities at high Re, and of Orr (right) who uses a spherieal eoordinate system fixed to an aetual sphere. Both studies make extensive approximations of initial eondition data that are quite uneertain.

The second technical approach is to advance the state-of-the-art numerical solutions to a state where turbulent initial conditions emerge in a pre-existing stratification, just as in experiment. Then, we search for meaningful way to make quantitative comparison.

3. Results summary

(i) Experimental techniques — RIM

Experiments have been conducted in Refractive-Index-Matched fluids at Re = 2.2 x 10^4 and Fr = 10. The first series of tests show that the RIM technique works, and identifies the source of the RI variation, and how it appears as a pseudo-velocity field (e.g. Fig. 4).

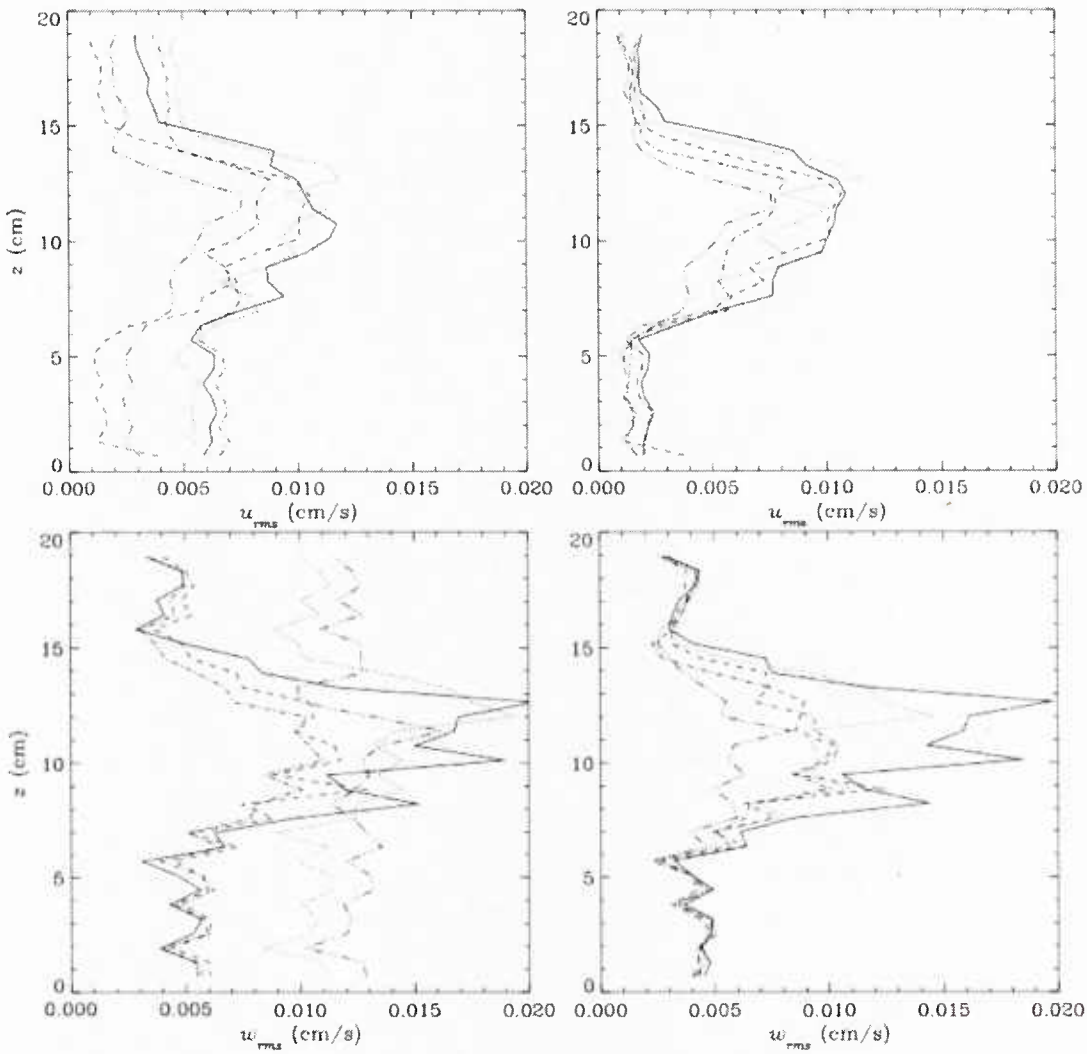

Fig. 4: RMS disturbance profile evolution in non-RIM stratified environment. $Nt \approx 0$ (--▣▣▣--), 0.17 (--▣--▣--), 0.34 (dashed), 0.52 (dotted), and 2.58 (solid) from a single experiment. The left column is uncorrected and the right is corrected. The top row plots u_{rms} and the bottom row w_{rms}. All axis scales are the same.

The measurements in a confined tank show some finite depth and fetch effects (Fig. 4, left column) but these can be removed using quite simple far-field corrections (right column). The data show the early time evolution of fluctuating velocity components, but these are created only by optical RI variation. The RI variation is related, in some non-simple way, with the turbulence in the wake itself. Fig. 5 shows that the time-evolution of single-column disturbance profiles can be traced in time in the early wake. Fig. 5 then shows that this apparent velocity field can be completely removed through careful manipulation of the salt and alcohol concentrations

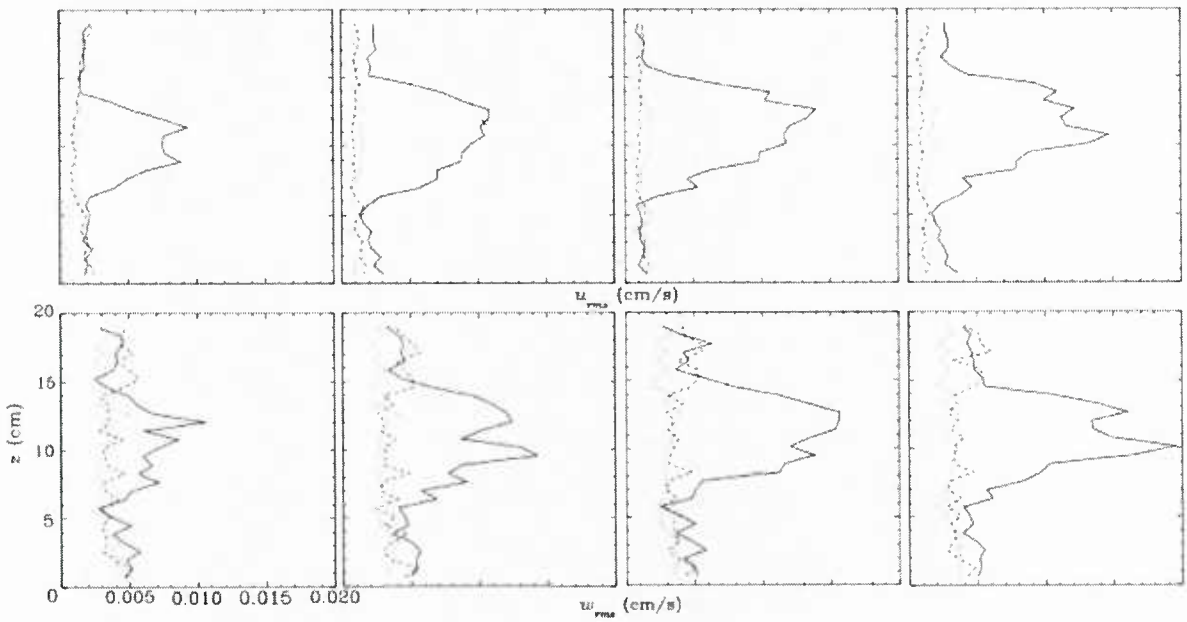

Fig. 5: RMS disturbance profiles compared for three fluid media: Non−RIM, salt-stratified (solid), RIM stratified (dotted) and pure water (dashed). Timesteps are $Nt \approx 0$, 0.52, 1.03, 1.89. The top row plots u_{rms} and the bottom row w_{rms}.

The uncertainty in velocity profile reconstructions, which ought to be uniform vertically, is about 10% of the peak disturbance quantity. The profile from pure water does not differ significantly, in any of the averaged quantities, from the RIM equivalent. We conclude that the technique works as predicted.

In statistically-stationary flows, it is reasonable to compile time-averages and look for convergence, which may also be achieved if the interval includes a sufficient number of instances of the non-stationary event. Moreover, late wake studies have made a transformation between dimensionless x and t as

$$\frac{x}{D} = \frac{Ut}{D} = \frac{Fr}{2} Nt \, .$$

Typically, experiments then compile data in streamwise averages over some finite distance, X, and these are treated as though they were time averages at a fixed Nt. This is plausible when the averaging distance, ΔX is a small fraction of the total wake length, X_W. The expression is

$$\frac{\Delta X}{X_W} = \frac{\Delta X/D}{Nt\,Fr/2}.$$

Clearly, when either ΔX or t is small the condition is not satisfied. This means that time averages at a single X location in body-frame coordinates is required to make a meaningful measurement. Even then we may not be sure that there is statistical convergence. Fig. 6 suggests that averaged profiles may exist, and even that similar shapes might be sought.

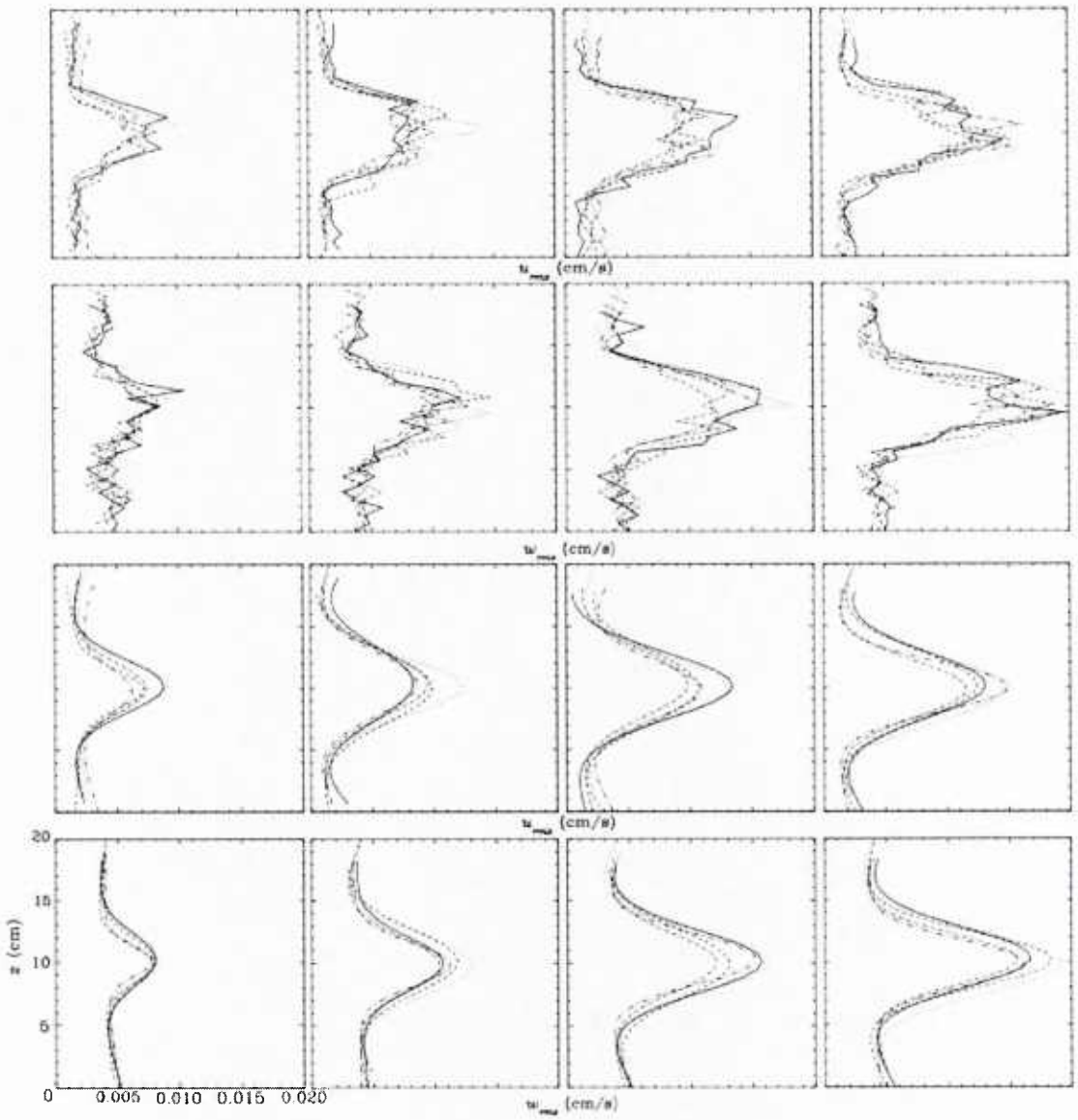

Fig. 6: Fits of the $u_{rms}(z)$ (row 1 and 3) and $w_{rms}(z)$ (row 2 and 4) velocity profiles in 5 repeated experiments for $Nt \approx 0$, 0.52, 1.03, and 1.89.

No single profile looks exactly like a Gaussian curve, but the existence of Gaussian solutions in the equations of motion is only postulated for time-averages of fully-developed turbulence. In the near wake such conditions may not exist. The lower two rows of Fig. 6 show that the search for Gaussian fits may not be entirely futile, though there is little analytical basis for this empirical finding. These profiles are equally reasonable in both streamwise and vertical velocity profiles. Continued experiments resulted in improved solutions, and the technique was tested extensively in a grid wake, where initial turbulence intensities were high..

(ii) Experimental techniques — parameter studies

Experiments were conducted in Refractive-Index-Matched fluids at a range of Fr and Re given in Fig. 7. The experimental parameters are matched so that a 3 x 3 (and 2 lower Fr) variation of Fr and Re were accomplished with 5 different values of the density gradient. Each experiment was repeated at least 16 times and multiple averages (up to 900) are used to make local time-averages in a reference frame that moves with the grid. Extensive results have been taken for the particular case of a towed grid. Two main points have emerged: (1) There are no other comparable data in the literature, even for such a canonical and basic problem. (2) Careful investigation and analysis shows there is no 3D regime in this case, and therefore such a regime cannot be either presumed or universal.

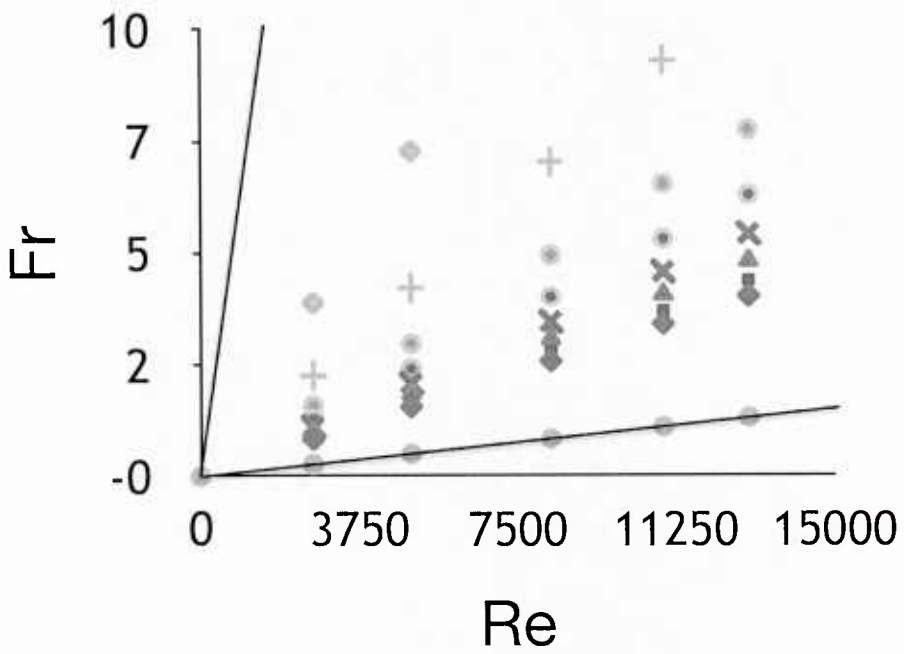

Fig. 7: Completed experiments with independent variation of Re and Fr

(iii) Experimental techniques — local statistical convergence

Fig. 8 shows that the time-averaged iso-vorticity contours have converged to a smooth final value within 100 independent samples. This is almost 1/10th of the total number of samples available from these experiments, and suggests that in future, wide-sweep parametric studies can be done with about 6 separate experiments, about 1/3 the number we have accumulated for this detailed test case.

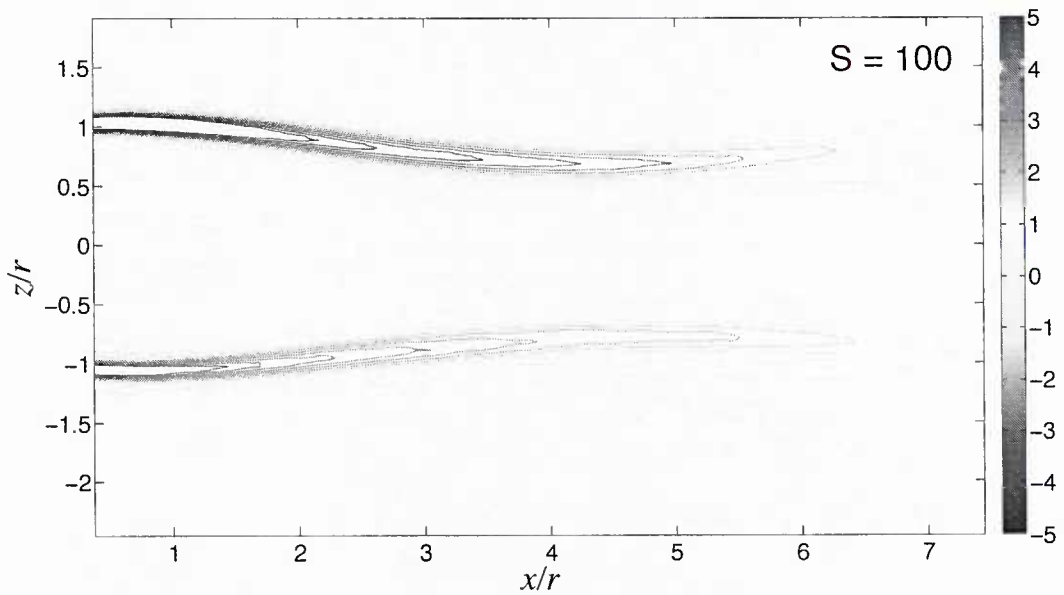

Fig. 8: Mean lateral vorticity contours for ensemble averages with n = 100.

Measurement here begin at $x/r = 0.6$, rather than zero because the grid geometry shades its immediate wake. The sphere will not have such a restriction. Note the shrinkage of the wake in the vertical direction, as it reaches its minimum value at x/r = 5. This feature has only ever been inferred from qualitative measurements before, most being visualizations of the integrated density field in shadowgraphs. Here the wake extent is measured purely in terms of kinematics of the flow field, and not through indirect evidence from refractive index variations averages across the wake.

Now that mean wake features are described, it is simple to show convergence of statistics in specific areas, such as along the wake edge defined by the vorticity extrema. Fig. 9 shows such convergence. By S = 100 (number of independent samples), the vorticity decay at the wake edge can easily be measured and parametrized.

Fig. 10 shows an initial estimate of the time evolution of averaged lateral vorticity profiles in the wake. The evolution is completely smooth and gradual. It is surprising to see such rapid convergence in the near wake, and it is a consequence of the particular initial conditions. The importance and persistence of initial condition information has been a central focus of this project.

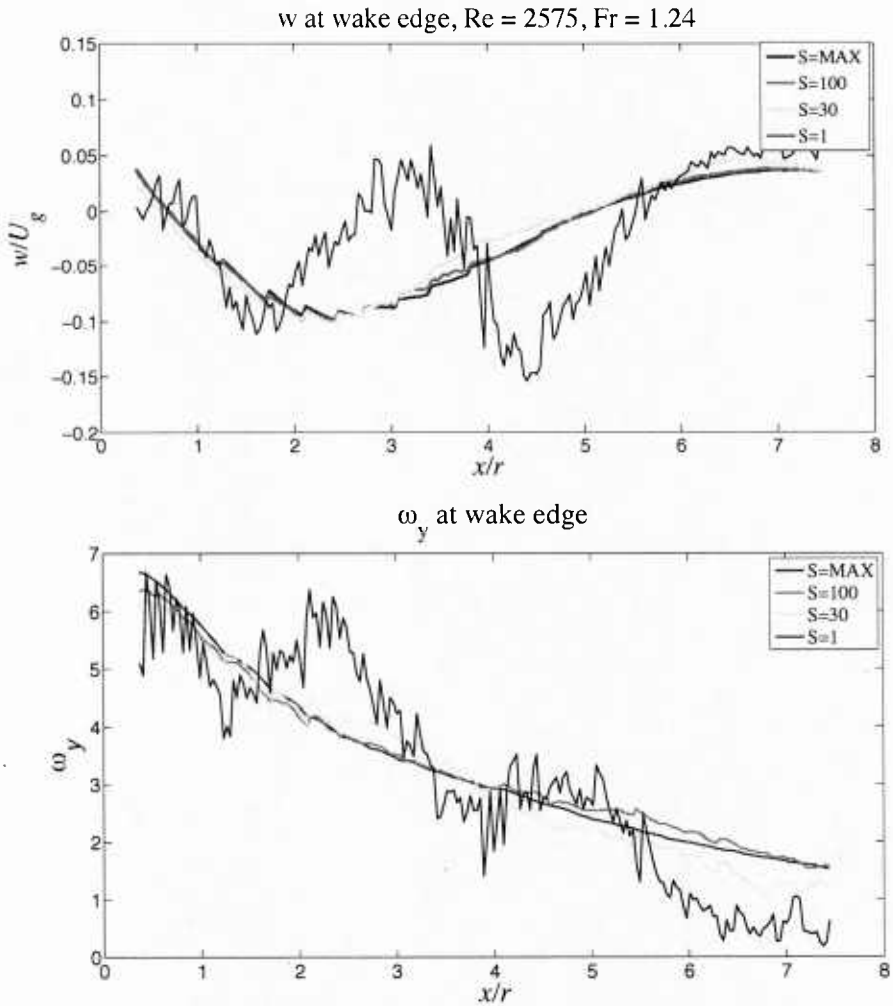

Fig. 9: Convergence of the vertical velocity and of the lateral vorticity time averages as a function of number of independent samples, S.

Finally, Fig. 11 shows one possible measure of structural information from an instantaneous lateral vorticity plot, and then a power spectrum averaged from 20 spectra on independent timesteps.

Again, such measures should be valuable in making detailed comparisons with numerical experiments.

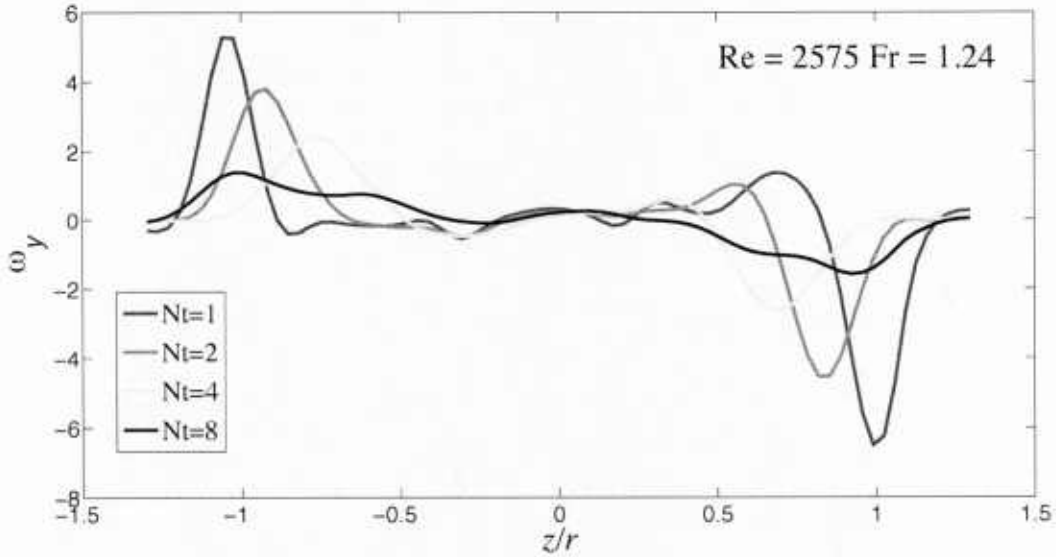

Fig. 10: Lateral vorticity profiles in the early wake. The transition from Nt = 1 to Nt = 5 is gradual.

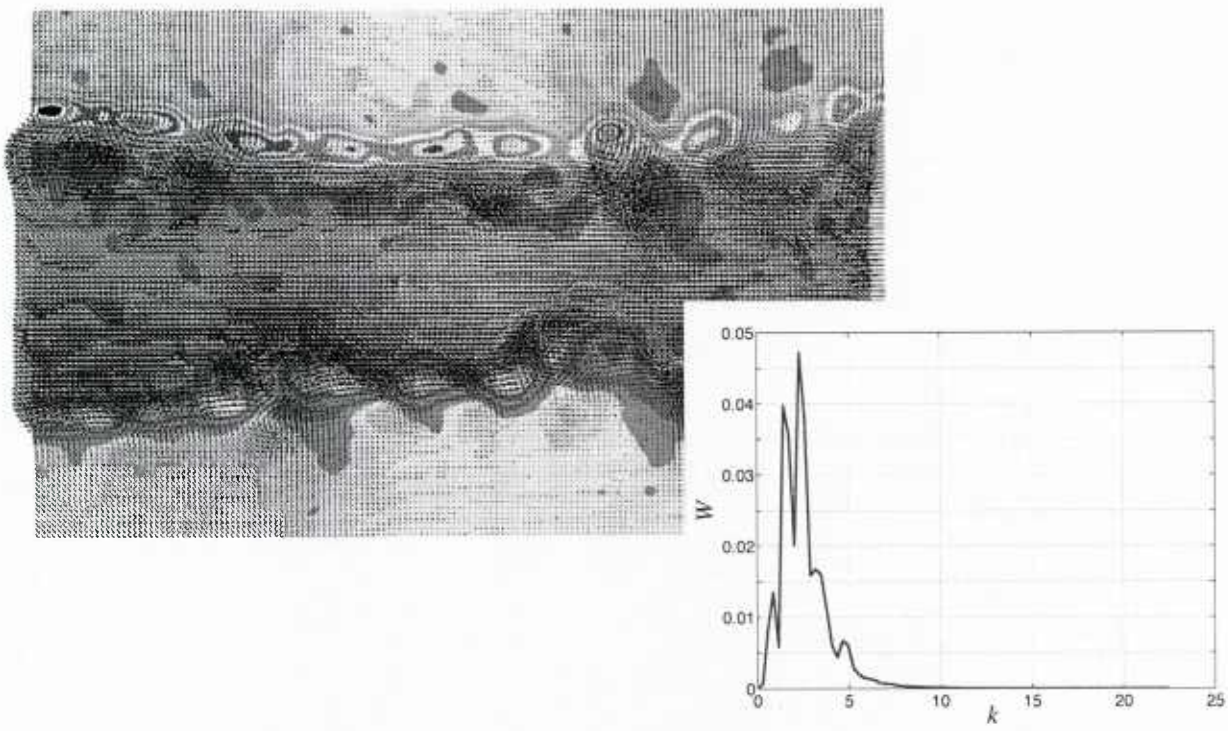

Fig. 11: Using a line defined by the time-averaged vorticity, a power spectrum (inset) taken along the wake edge shows scales from the coherent structures and from their subharmonic.

(iv) Experimental techniques — quantitative studies

The most detailed analysis was performed on the early wake behind a towed, square grid, and a typical time series is shown in Fig. 12.

The data show how, in the time-averaged sense, there is a consistent inflow-outflow pattern behind the grid at Nt = 4. The streamwise velocity accelerates behind the narrow necking after the grid, and the vertical mean shows an extent into the far-field. The larger scale structures in the vertical mean also have wavelengths similar to Nt = 4. When the mean vertical velocity is

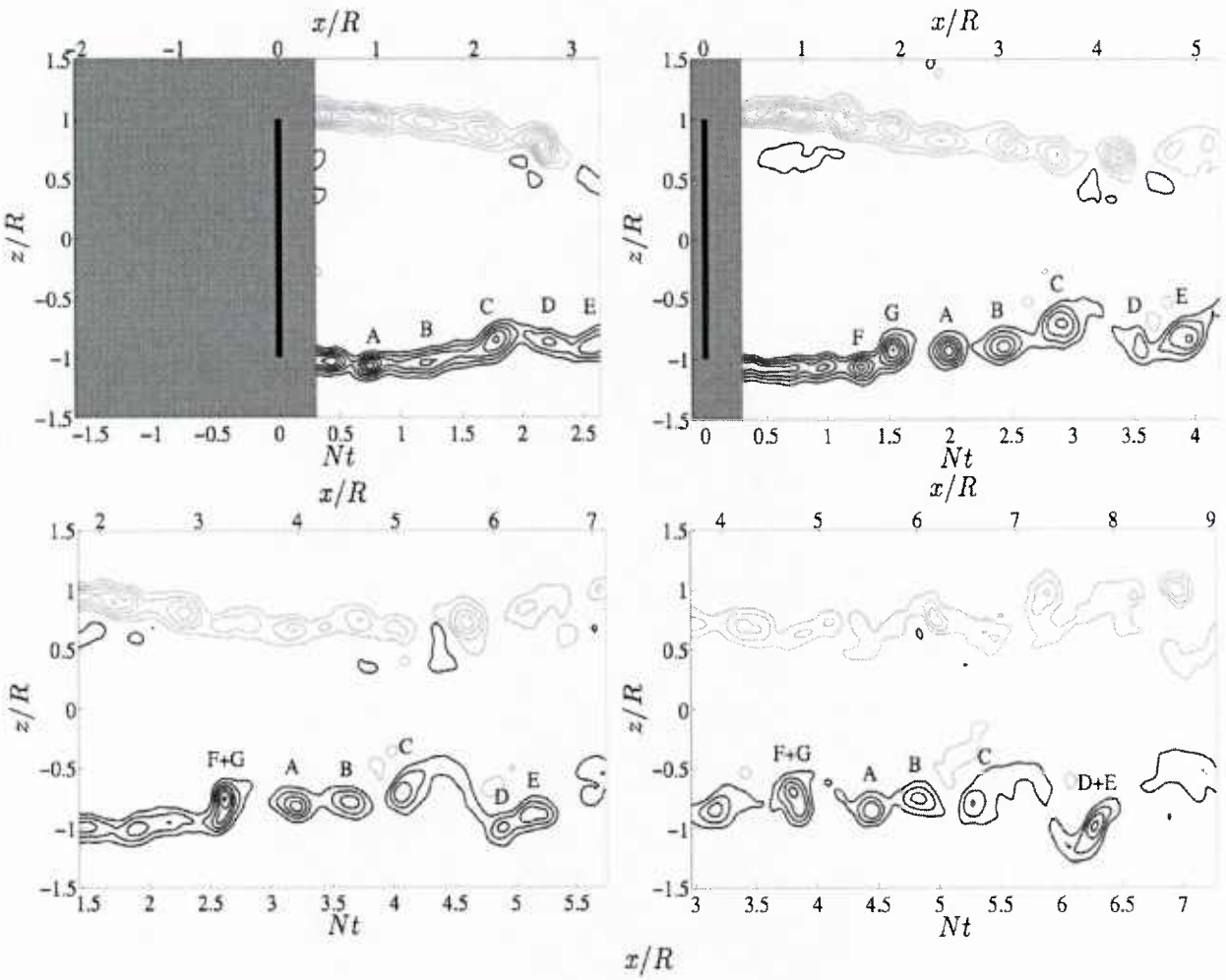

Fig. 12 Time series of instantaneous lateral vorticity behind the grid. Individual vortices are labelled and can be tracked.

removed, the remaining component shows the contribution at the wake edge form the vortices alone. These vortices therefor do not move at the grid speed, but at some different (slower) speed.

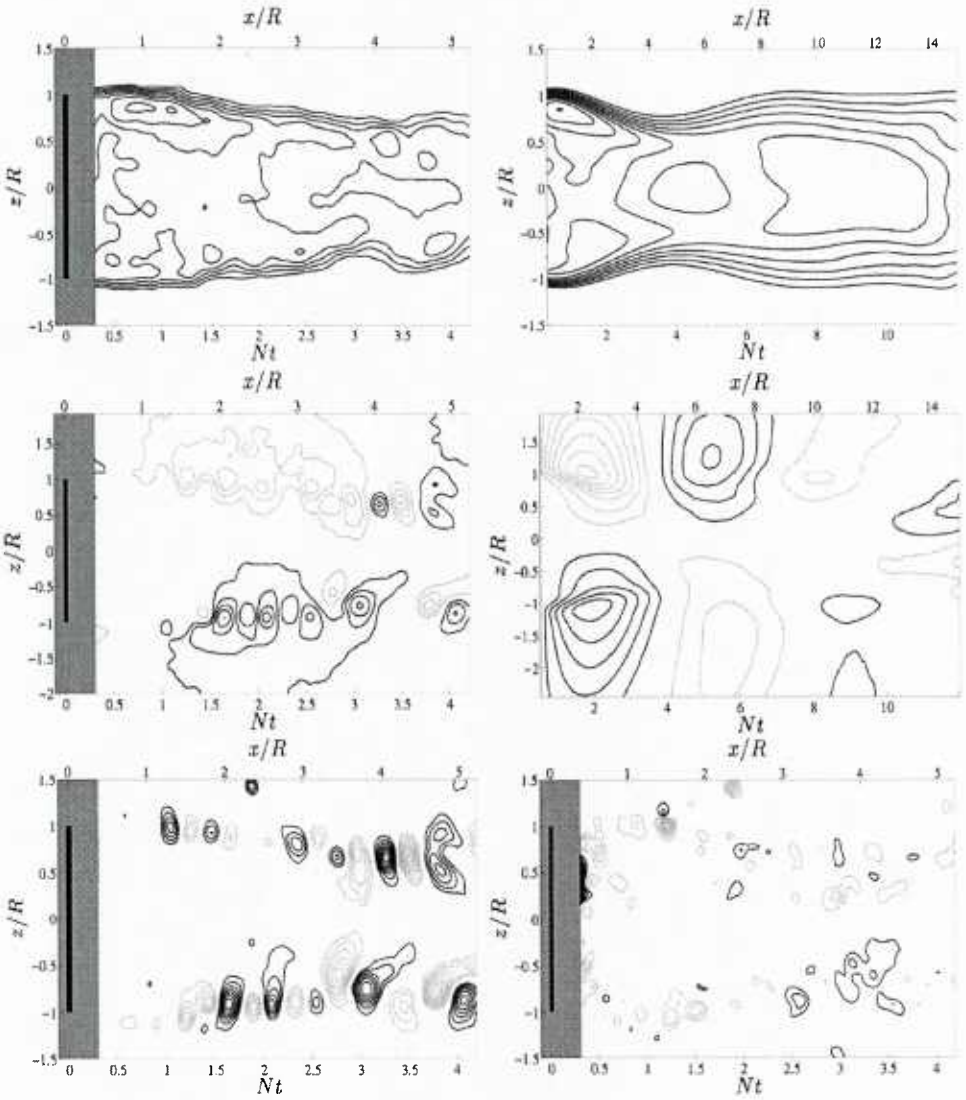

Fig. 13. Instantaneous and time averaged streamwise velocity (top row), vertical velocity (middle row) and instantaneous vertical perturbation velocity, and lateral velocity for one time instant (bottom row).

Fig. 13 shows a single, instantaneous streamwise velocity field in the top left corner. Time averages for a number of quantities (mean U, mean w, and mean W) are given in the next 3 panels. The lower frames show the perturbation vertical velocity, w, and the out-of-plane component, v. The individual vortices are generated at the wake edge shear layers, and the flow field itself represents an interesting balance between instability of strong shearing motions ta the wake edge and large scale coherence due to buoyancy which sets the lee wave length see in the top row of Fig. 13.

Local measures can be made of the lee wave characteristics, and Fig. 14 shows one example where the fluctuating velocity component at the wake-edge (Fig. 13e, also defined by peaks in the vorticity magnitude, Fig. 12) is measured as a function of downstream distance.

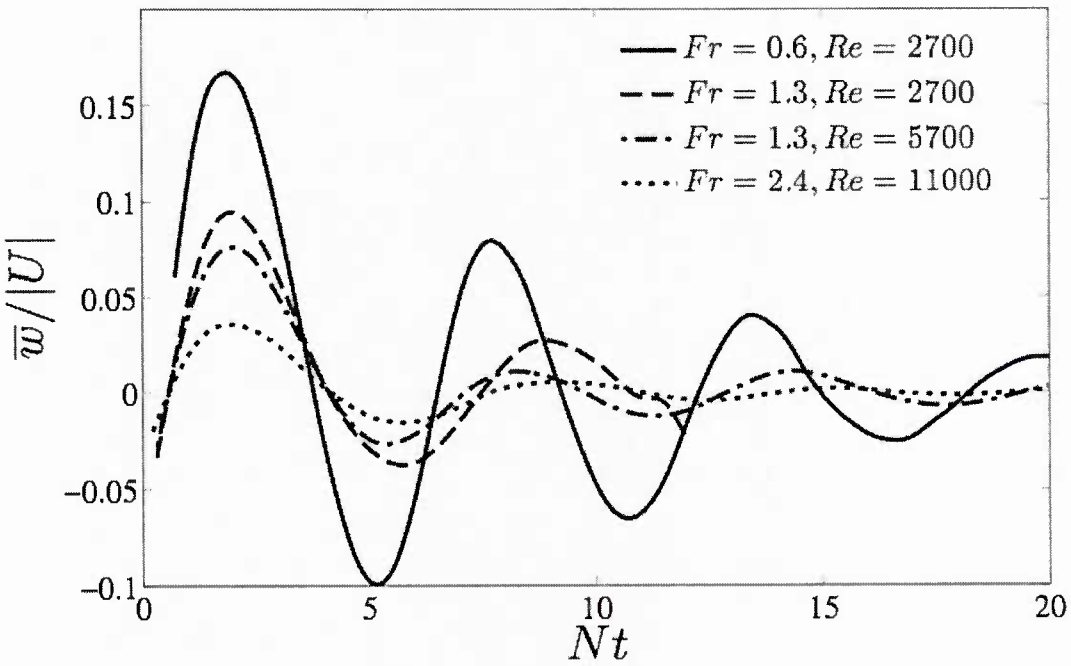

Fig. 14. Mean fluctuating velocity at the wake edge.

The variation in observed wavelength with Fr and Re is consistent with what would be seen in lee waves behind a bluff body. The agreement with existing data from laboratory and numerical experiment of sphere wakes is very good (Fig. 15). The rectangular grid is a convenient mechanism for producing arbitrary turbulence intensities with respect to the mean flow and background density gradient, and it is quite interesting to see how at this solidity it has common characteristics with sphere wakes too.

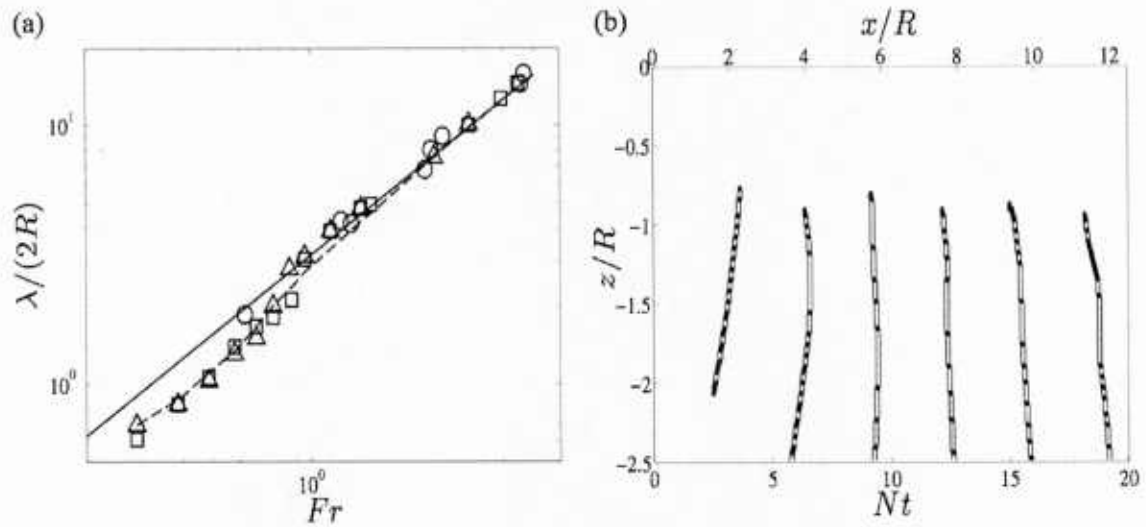

Fig. 15. (a) Wake-edge wavelength as a function of Fr. Solid line is linear theory. Symbols are laboratory and numerical experiments on spheres. (b) Lee wave isophase lines.

This one experiment therefore has some tunable characteristics that allow it to be used as a platform for a number of different test cases.

The sphere wake has been claimed (by us) to have many universal characteristics. In the late wake we have direct evidence for this claim, but we have none in the early wake. Fig. 16 shows that there can be no universal regime, at any time.

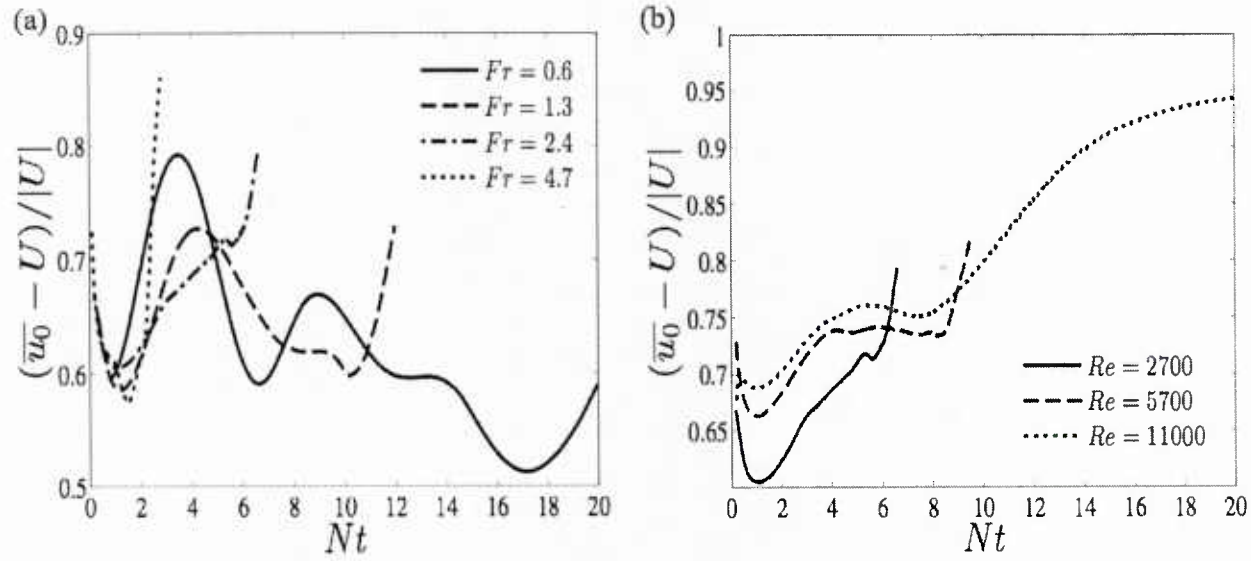

Fig. 16. (a) Mean fluctuating centerline streamwise velocity for varying Fr at Re = 2700, and (b) for varying Re at Fr = 2.4.

The mean fluctuating streamwise velocity comes from removing the centerline component of the mean flow. Note how the result is expressed relative to the moving grid. An initial dip is followed by a peak as the flow locally accelerates. The magnitude of this effect clearly varies with Fr. At Fr = 2.4, the low Re case does not align with the other two. No single scaling can account for the local behavior, and at no time is the flow independent of Fr. This result holds up to Fr = 10 (not shown). At some Fr, one might imagine that the near wake flow would proceed as if there were no background stratification, but we have not found that Fr yet, and in any event such a scenario directly contradicts the notion of a universal wake.

The dependence on Fr and Re now gives new cause for thought in attempting to scale the wake results. A single example is shown in Fig. 17, where the lateral vorticity is plotted against Nt.Fr/Re, which is vt/R^2. The initial value is arbitrary, and its unscaled value varies with Fr, but not in an easily reconcilable way. A scaling with vt/R^2 is a little like 1/Re, and suggest a viscous/inertia balance set by the grid parameters, with the implication being that stratification is unimportant in the developing shear layer at the wake edge. The scaling rationale is not yet clear and does not accord with known late wake scalings.

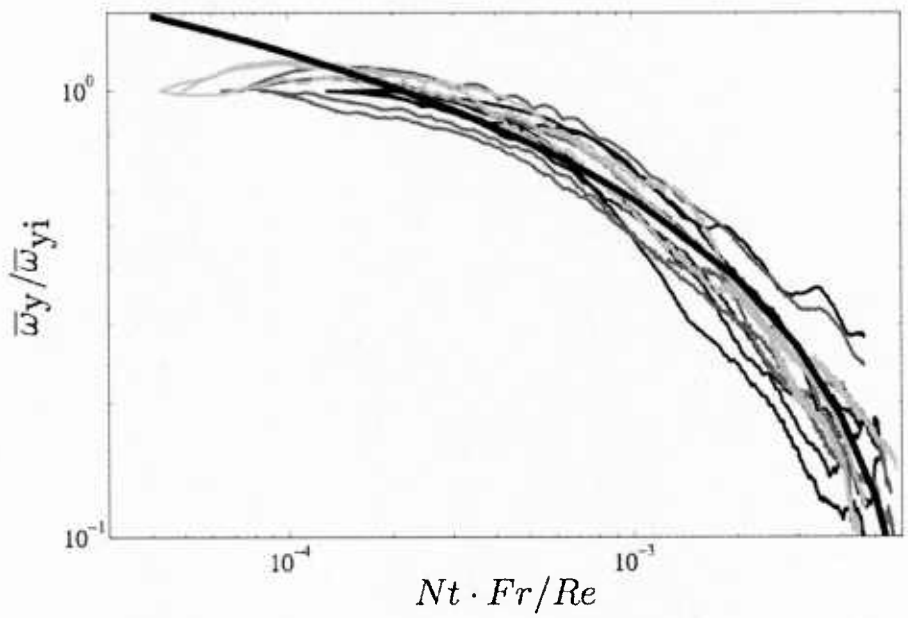

Fig. 17. Decay of rescaled vorticity at the wake edge. The thin black lines, dark gray lines, and light gray lines are for Re = 2700, 5700 & 11000. The thick black line is a logarithmic curve fit.

Though viscosity seems important at the wake edge, it is not necessarily always dominant, and the flow can go through inviscid instabilities and the generation of turbulent fluctuations at a number of locations in the wake.

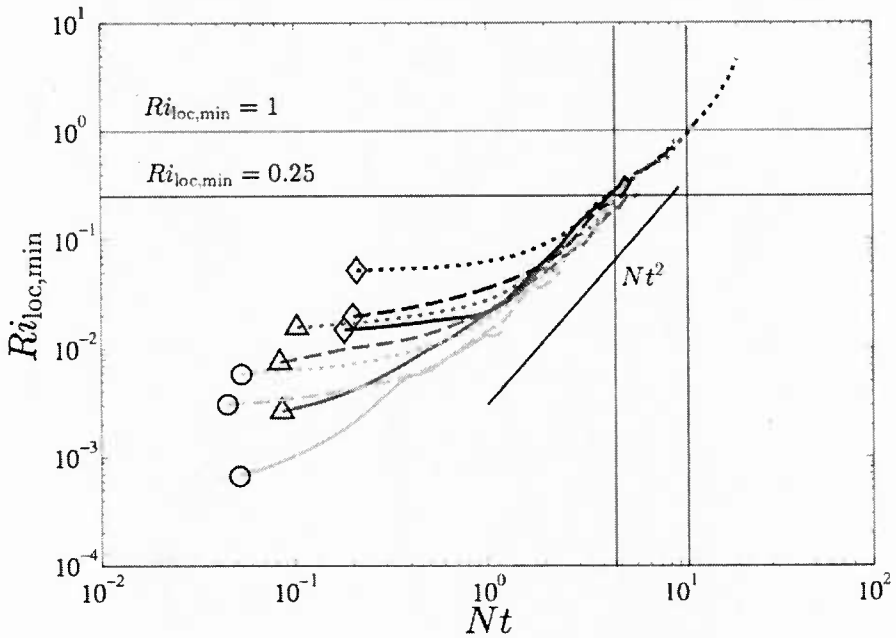

Fig. 18. The local minimum Richardson number for Re = {2700, 5700, 11000} and Fr = {2.4, 4.7, 9.1}.

A local Richardson number can be written as $Ri = N^2/S^2$, where S^2 is the mean square local shear. When Ri is small the flow can be unstable, and a criterion for this is $Ri < 1/4$. Sometimes in the stratified flows literature a threshold of $Ri = 1$ is given.

In Fig. 18, the initial minimum Ri is always less than 1/4 and the Ri(Nt) curves collapse onto a Nt^2 line before $Ri > 1/4$. The measured dependence on initial Fr is the same as that reported by [Di11]. For constant Fr, larger Re gives larger initial $Ri_{loc,min}$, which is now opposite to [Di11]. We note here that numerical and laboratory experiments differ fundamentally in the way in which certain parameters are varied. To vary Re, a numerical experiment simply varies v, with no other change. Constant Fr corresponds to constant U, N and L. In an experiment, v is not an independently-controllable parameter, and when U is increased to increase Re, then N must increase by the same amount so as to keep $Fr = U/NL$ fixed. Thus, our variation in Re is always accompanied by a variation in N to set the initial Fr. If scale similarity is not maintained (and there is no a priori reason to believe it would be) in the early wake, then local Fr, depending on local scales of U and L, and which presumably do set the dynamics of the flow, can behave differently.

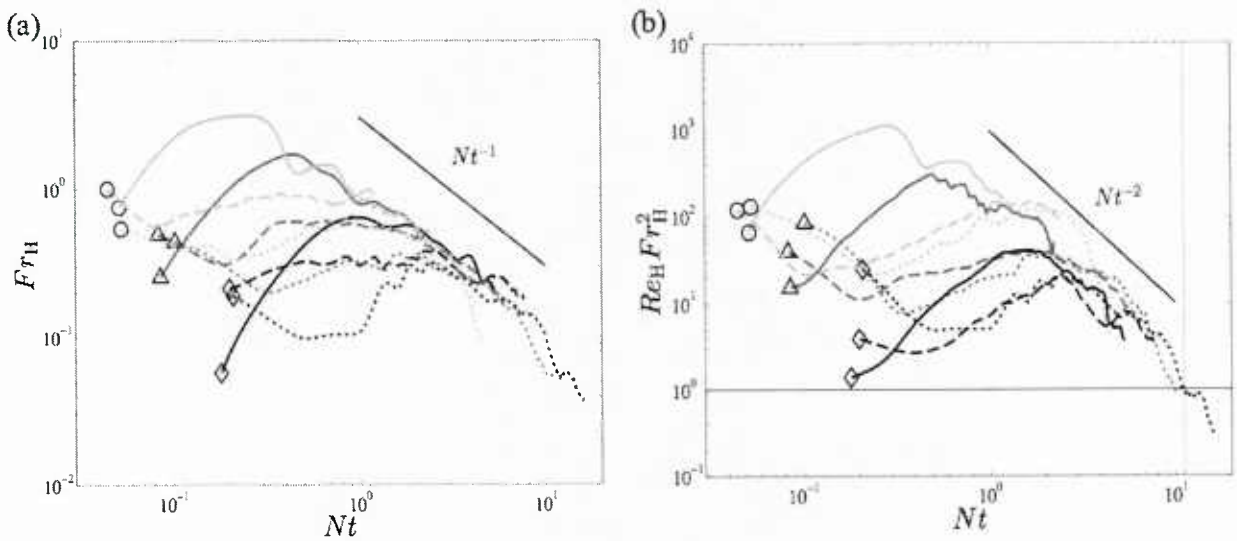

Fig. 19. The evolution of (a) a local horizontal Froude number, FrH and (b) the buoyancy Reynolds number.

In Fig. 19, Fr_H and $Re_b = Re_H.Fr_H^2$ show variation with initial Fr and Re in quite complex ways. The experiment achieves short periods where Re_b exceeds 10, and so in the sense of [Ri03, He06] we may conclude that we are in a stratified turbulence regime that has not yet been quenched by viscosity. This means that the current findings of curious, non-universal scaling behavior need to be accounted for, in future experiments and numerical simulations.

(iii) Numerical experiments

Though the research proposal focussed primarily on experiments, and we do not conduct numerical simulations ourselves, part of the point of the research is to make these close connections with the relevant groups. These are: Domaradzki (USC); Diamessis (Cornell); Sarkar (UCSD). Here we briefly note some recent results from Orr & Domaradzki, since we have been closely involved, and we will point out only selected cases where experiments have a particular interest or role to play.

The simulations were conducted on a grid that includes the sphere itself, as shown in Fig. 3b. Fig. 20 shows that the simulation results are consistent with previous data in near wake studies, including lower Reynolds number simulations (Hanazaki, Rottman et al.) and experimental work of Lofquist & Purtell.

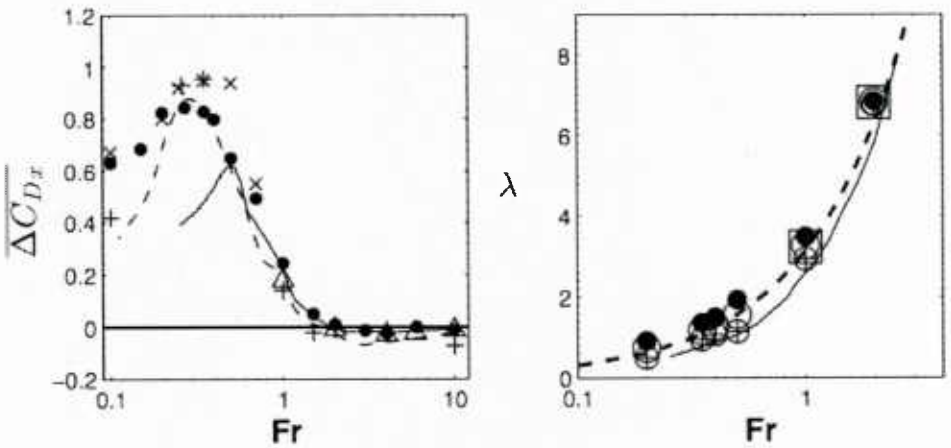

Fig. 20: (a) Change in stream-wise drag coefficient due to stratification. (–) Hanazaki, (––) Lofquist & Purtell, { × (low-res), + (med-res)} Rottman *et al.* , current simulations at (•) Re=200, △ Re=1000. (b) Calculated λ: (–) Hanazaki, (––) linear theory, current simulations {⊕,○,•} at z = {0.5, 1.0, 1.5} for Re=200, at z = 1.0 for Re=1000.

There are some discrepancies between the low Fr simulations and those of Hanazaki. The reasons have yet to be worked out. The result shows that certain results are consistent in the literature but that some are not. This presents an interesting challenge and opportunity for future work.

The numerical experiments allowed for an interesting investigation as to the effects of finite space averaging techniques, and mimicking PIV sampling conditions in a moderately near wake (Fig. 21) shows that experimentally-derived velocity profiles have features in them that can only be matched if similar pseudo-sampling strategies are followed.

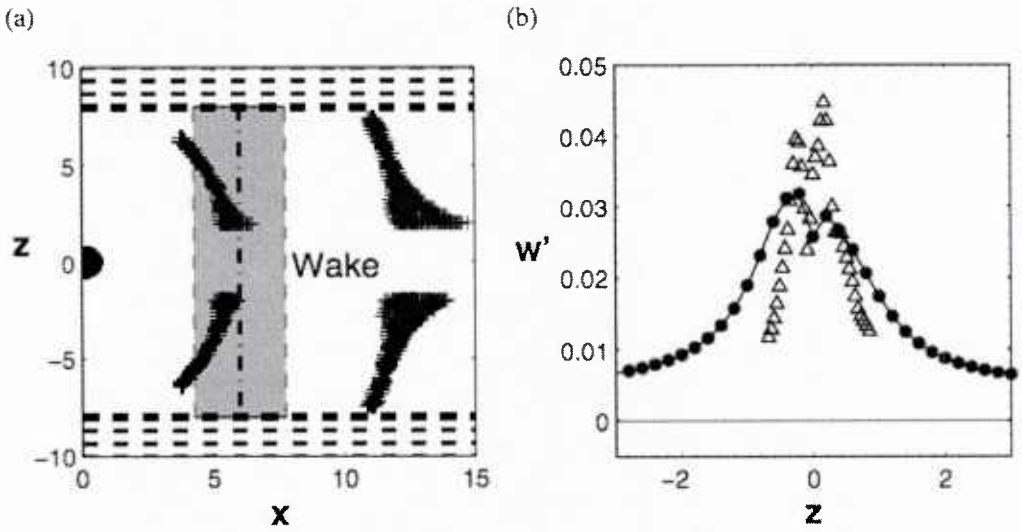

Fig. 21: Re = 1000, Fr = 4. (a) Shaded area is DPIV window centered about x_{wc} = 6, sphere at (x, z) = (0, 0) is moving to the left, (—) damping layer. (+) detected locations for |z| > 2 and 3.75 ≤ x ≤ 14.75 where w′ $(\vec{x}, t)$ 10^{-3} = 0 over ΔT = 40, sampled at Δt = 0.4. (b) (– · –) Simulation comparison w′ (x_{wc}) with (△) Re = 5000 experimental w′ (x_{wc}, T).

The form of Fig. 21b is inevitable in any finite-length wake sampling program, and this match will be investigated for profiles of the form of Fig. 21 in the future.

No new high-resolution simulations have been carried out in the last year, but the data from Orr's computations have been collected and summarized. As an example, Table 1 shows the parametrization and prediction of all stratified sphere wakes in the vertical direction for various quantities, q, as given by

$$\left.\frac{q(x,z)}{q_o}\right|_{Fr} = \exp\left[-\frac{(z/L_{\sigma v}-B_z)^2}{C_z^2}+\frac{B_z^2}{C_z^2}\right] + \exp\left[-\frac{(z/L_{\sigma v}+B_z)^2}{C_z^2}+\frac{B_z^2}{C_z^2}\right]$$

	U/U_o		u'/u'_o		v'/v'_o		w'/w'_o		ρ'/ρ'_o	
Fr	B_z	C_z	B_z	C_z	B_z	C_z	B_z	C_z	B_z	C_z
4	0.00	0.69	0.54	0.50	0.00	1.18	0.00	1.02	0.00	0.95
6	0.00	0.72	0.62	0.54	0.00	1.16	0.00	1.07	0.00	1.24
10	0.00	0.74	0.58	0.52	0.00	1.08	0.00	1.12	0.00	1.43
∞	0.00	0.73	0.62	0.60	0.00	0.98	0.00	1.31	n/a	n/a

Table 1: Predicted profile shapes in z for mean and fluctuating velocity components, and for the density fluctuations.

The predictions are quite explicit, and quite adventurous. It will be very helpful to compare them with experimental data at exactly the same Reynolds number.

4. Plans

The primary objective and realizing detailed experiments on early wakes was successful. In doing so, we have over-turned one of the canonical results in the literature for we ourselves have been most responsible. It is clear that no universal stage occurs in stratified turbulent early wakes and the main question now becomes: what happens to this initial-condition specific information? What happens to it so the late wake scaling can ignore it? What are the necessary and sufficient conditions for preservation of information into late stages? We are now at an excellent point to make very specific comparisons in repeated runs with numerical data, which have now been published. This will allow us to understand whether we are indeed simulating the same environment in laboratory and numerical experiments. When and if we are, then we will be justified in making archival and multi-parameter databases.

5. Publications

References

[Br10] Brucker KA, Sarkar S. 2010. A comparative study of self-propelled and towed wakes in a stratified fluid. *J. Fluid Mech.* **652**, 373-404.

[Di11] Diamessis PJ, Spedding GR, Domaradzki JA. 2011. Similarity Scaling and Vorticity Structure in High Reynolds Number Stably Stratified Turbulent Wakes. *J. Fluid Mech.* **671**, 52-95.

[Do02] Dommermuth DG, Rottman JW, Innis GE, Novikov EA. 2002. Numerical simulation of the wake of a towed sphere in a weakly stratified fluid. *J. Fluid Mech.* **473**, 83–101.

[Go01] Gourlay MJ, Arendt SC, Fritts DC, Werne J. 2001. Numerical modeling of initially turbulent wakes with net momentum. *Phys. Fluids* **13**, 3783–802

[He06] Hebert DA, de Bruyn Kops SM. 2006. Relationship between vertical shear rate and kinetic energy dissipation rate in stably startified flows. *Geophys. Res. Lett.* **33**, L06602.

[Me04] Meunier P, Spedding GR. 2004. A loss of memory in stratified wakes. *Phys. Fluids* **16**, 298-305.

[Me06a] Meunier P, Spedding GR. 2006. Stratified propelled wakes. *J. Fluid Mech.* **552**, 229-256.

[Me06b] Meunier P, Diamessis PJ & Spedding GR 2006 Self-preservation in stratified momentum wakes. *Phys. Fluids* **18**, 106601

[Or15] Orr TS, Domaradzki JA, Spedding GR, Constantinescu, GS. 2015. Description of the near wake of a sphere moving in a steady, horizontal motion through a linearly stratified fluid at Re=1000. *Phys. Fluids* (in press)

[Ri03] Riley JJ, de Bruyn Kops SM. 2003. Dynamics of turbulence strongly influenced by buoyancy. *Phys. Fluids* **15**, 2047-2059.

[Sp96] Spedding GR, Browand FK, Fincham AM. 1996. Turbulence, similarity scaling and vortex geometry in the wake of a towed sphere in a stably-stratified fluid. *J. Fluid Mech.* **314**, 53-103.

[Sp97] Spedding GR. 1997. The evolution of initially-turbulent, bluff-body wakes at high internal Froude number. *J. Fluid Mech.* **337**, 283-301.